

Blue Straggler Stars in Galactic Open Clusters and the Simple Stellar Population Model

Y. Xin^{1,2}, L. C. Deng² and Z. W. Han¹

xinyu@bao.ac.cn

ABSTRACT

Blue straggler stars present as secure members in the Galactic open clusters form a major challenge to the conventional picture of evolutionary population synthesis based on the stellar evolution theory of single stars, as illustrated in our previous work. Expansion of our sample in the current work to include younger age clusters provides a larger data base to expose the question raised for the simple stellar population model. The working sample now includes 97 Galactic open clusters of ages ranging from 0.1 to several Gyrs. The contributions of blue straggler stars to the integrated light of the host clusters are calculated on an individual cluster base. A data base of observational constrained simple stellar population model is made which has a larger age coverage than our previous work. It is shown in this work that the general existence of blue stragglers in star clusters of our sample dramatically altered the predictions of conventional stellar population model in terms of spectral energy distribution. The integrated spectral energy distributions of the synthetic spectra of the clusters are enhanced towards shorter wavelengths, therefore the results of the present work will cast new lights in understanding the properties of stellar populations.

Subject headings: blue stragglers — open clusters and associations: general — Galaxy: stellar content

1. INTRODUCTION

Although the evolutionary population synthesis (EPS) method has been widely applied in analyzing stellar contents of local and remote galaxies, and has been proved to be very successful in many aspects, there are still some fundamental problems indeed in the framework

¹National Astronomical Observatories/Yunnan Observatory, Chinese Academy of Sciences, PO Box 110, Kunming, Yunnan Province, 650011, China

²National Astronomical Observatories, Chinese Academy of Sciences, Beijing, 100012, China

of EPS. One of the challenges to the EPS is that the effect of complex stellar interactions which are common in all stellar systems, such as mass exchanging and coalescence in binaries and collisions between single and/or binaries, etc., is not considered in the method. The conventional picture of EPS is mainly based on the single-star evolution theory and is performed with the evolutionary behaviors and spectra libraries of individual stars (Bressan et al. 1994).

In order to attack such a problem, getting direct observational spectra of simple stellar populations (SSPs) had been practiced by former studies, such as the early work of Bica & Alloin (1986a, b). They undertook a direct approach using the observational integrated spectra of star clusters, assuming that these clusters are SSPs so that the EPS can be constrained observationally. Direct observation of star clusters is a meaningful approach to discuss the integrated properties of SSPs, and it is free of any assumptions about the initial mass function (IMF) and the details of stellar evolution. However, such a treatment can not perfectly reproduce the conventional SSP model, since the dynamical evolution of star clusters has modified the content of the original population, such as gravitational evaporation of low-mass member stars. More importantly, possible foreground star contaminations to the spectra cannot be assessed in an ideal manner. A practical way out should be resolving member stars photometrically using proper motion and/or radial velocity data. By conventional SSP model through this paper, we mean that the model is built based on single star evolution theory.

We have carried out a plan to attack this problem semi-empirically. The Galactic open clusters (OCs) are taken as our working sample to explore the contributions of blue straggler stars (BSs) to the conventional SSP model. The first set of results for old OCs with ages greater than 1Gyr has been published (Xin & Deng 2005, hereafter XD05). All the member stars within a cluster are presumably born at the same time from the same origin, therefore should have the same age and metallicity. Star clusters have been long regarded as one of the best objects to study the population synthesis technique (Battinelli et al. 1994). As described in XD05, the bulk of cluster member stars well fitted by an isochrone represents the idea of conventional SSP model. All the other member stars straggling away from the isochrone belong to the same population, no matter how weird their positions in the color-magnitude diagram (CMD) are, and have to be included when considering the integrated light properties of the population. Among the stragglers, BSs are of special interest because they are the only luminous objects straggling away from the predictions of the theory of single star evolution. It is also important to recall that these bright objects cannot be fully understood either by current theory of binary star evolution. Baring these in mind, the semi-empirical model used in XD05 is still a working approach. Besides, the nature of BSs is a challenging subject of stellar evolution, which is under active investigations (Tian et al.

2006, Hurley et al. 2005, Chen & Han 2004).

Since the first identification of BSs by Sandage (1953) in the globular cluster (GC) M3, the common existence of this kind of stars has been proved in stellar systems of all scales and complexities (e.g., Ahumada & Lappaset 1995 for open clusters; Piotto et al. 2002 for globular clusters and Lee et al. 2003 for dwarf galaxies). The typical locations of BSs in the CMD of a cluster are at the bluer and brighter extension of the turnoff point of the host cluster, therefore they are the most luminous and bluest hydrogen burning stars of the cluster at the time of observation (Deng et al. 1999). The main formation mechanisms of BSs are generally related with dynamical interactions of close binaries (Pols & Marinus 1994) and stellar collisions in the high-density areas (Ferraro et al. 2003). Therefore, statistical studies of BS populations in clusters in terms of integrated light provide a clue to such stellar interaction processes, and a reference to approaches such as binary evolution and dynamical evolution within the cluster, and eventually make the EPS more realistic. A larger sample is definitely needed for this purpose.

97 Galactic OCs are studied in this paper in terms of integrated light. A short description of the working sample is given in the next section. In §3, how BSs influence the integrated properties of conventional SSP model is discussed. The synthetic clusters' ISEDs involving BSs contributions show significant enhancements towards shorter wavelengths, especially in ultraviolet (UV) and blue bands, and consequently the integrated (U-B) and (B-V) colors become bluer. When measured with the modifications in (U-B) and (B-V) colors, the physical parameters of OCs, especially age and metallicity, show great uncertainties. The uncertainties are considered in more details in §4. The synthetic integrated spectral energy distributions (ISEDs) of our sample OCs are fitted with those of the conventional SSPs of either younger ages or lower metallicities. Based on the results of all the sample OCs, the uncertainties in measuring the fundamental parameters of SSPs are discussed. Finally, the concluding remarks on this work are presented in §5.

2. The Working Sample

In XD05, relying on the definite identifications of BSs and cluster turnoff point, we put our attention on the old Galactic OCs since they possess sufficient number of stars for good statistics and well populated all evolutionary stages. However, since the aim of this series work is to detect the effect of BSs quantitatively and systemically at ranges as large as possible in age and metallicity, a large enough working sample is inevitably needed. The working sample is expanded from 27 old Galactic OCs (age ≥ 1.0 Gyr) in XD05 to 97 Galactic OCs in this work, including 62 intermediate ($0.1 \text{ Gyr} \leq \text{age} < 1 \text{ Gyr}$) and 35 old

(age ≥ 1 Gyr) clusters.

The basic parameters of the sample OCs are given in Table 1, where column 1 is cluster name; columns 2-4 give the age ($\log(\text{age})$), color excess ($E(B-V)$) and distance modulus (DM); columns 5-6 give the metallicity (Z) and the $[\text{Fe}/\text{H}]$ values; columns 7-8 are the N_2 (number of stars within two magnitudes below the turn-off) and N_{BS} (number of BSs) numbers of the sample clusters. References for parameter adopted in this work are listed in column 9.

In order to keep the criterion homogeneous for selecting BSs in the clusters, we use exclusively the photometric data from Ahumada & Lappaset’s BS catalog (1995, hereafter AL95). N_2 and N_{BS} numbers are also from the same source. N_2 is defined as the number of stars within two magnitudes interval below the turnoff point of the host cluster. The detailed explanation of N_2 number can be found in XD05. The physical parameters of sample clusters, including age, $E(B-V)$, Z and DM, are mainly extracted from more recent literatures, the latest photometric data of the OCs are then used in this work in order to get optimistic parameters of the OCs and to select the BSs candidates in each cluster based on the observed CMDs more reliably. For sample OCs without accurate photometric data, the physical parameters are chosen in such a way that locations of majority of BSs are reasonable in the CMDs. Detailed derivation for every parameter is listed in Table 1.

The metallicity of a cluster is usually given as $[\text{Fe}/\text{H}]$ based on spectral observation and abundance analysis, but we need the information in Z to build conventional SSPs. In such circumstance, an empirical relation between Z and $[\text{Fe}/\text{H}]$ (Carraro et al. 1994) is adopted in the work,

$$\log Z = 1.03 \times [Fe/H] - 1.698. \quad (1)$$

When metallicity Z is marked as “0.02?” for a cluster in Table 1, it means that there is nothing available on metallicity for that cluster. In this case, we assume solar metallicity ($Z=0.02$) for it. The Galactic OCs generally possess younger ages and locate closer to the Galactic plane when compared with the Galactic GCs, which means that, at the first approximation, the assumption of $Z=0.02$ will not cause any essential errors for clusters considered in this work.

Figure 1 shows the number distributions of total 97 selected OCs as functions of four different parameters: $\log(\text{age})$, Z , N_{BS} and N_{BS}/N_2 . Only the clusters with published metallicities are used to plot the distribution in Z . As shown in the figure, most of our sample OCs possess Z values around $Z=0.02$, pretty much like what we expected, and hence it is an observational support to our assumption of $Z=0.02$ for the sample OCs without accurate metallicity determinations. The ratio of N_{BS}/N_2 can be regarded as a specific BS frequency

in a cluster. It can be used as a probe for the cluster internal dynamic processes concerning BSs formation. The three panels in Figure 2 show the correlations between N_{BS} and three different parameters: $\log(\text{age})$ (Figure 2a), Z (Figure 2b) and N_2 (Figure 2c), where there is no indication of obvious correlations between N_{BS} and $\log(\text{age})$, Z , even in this larger sample compared with the previous result in XD05. While a well defined correlation between N_{BS} and N_2 (Figure 2c) is clearly shown, which infers that BSs formation is quite similar in all OCs, and is positively correlated with the total number of stars. The BS content in a cluster is almost independent either of age or of metallicity of the host cluster.

3. MODIFICATION TO THE CONVENTIONAL SSP MODEL

As described in XD05, the stellar population corresponding to a cluster is assumed to be composed of two components. One accounts all member stars that are well fitted by an isochrone of single star evolution theory, i.e. a conventional SSP model. It is named as “SSP component” and its ISED can be directly built from theoretical model. The other component should include all the other member stars straggling away from that isochrone, and our attention is put only on BSs because they are bright. The other stragglers are not quite important in terms of contributions to the total light: the red stragglers in the middle of CMD are usually rare and less luminous; the underlopers and stars bluer than the main sequence but well below the turnoff are too faint to be important. The BSs fixed by photometric observations form the “BS component”. More detailed descriptions of model construction can be found in XD05.

In this work, the ISEDs of SSP components are extracted from the low-resolution conventional SSP model of Bruzual & Charlot (2003, hereafter BC03). The quoted ISEDs are built based on Padova isochrone (Bertelli et al. 1994), Salpeter IMF (Salpeter 1955) and Lejeune stellar spectra library (Lejeune et al. 1997). For details we refer BC03. The spectra of BS components are also made based on the Lejeune spectra library following a process of interpolation and fitting, see XD05 for details. Summing up the ISEDs of these two components, we get the synthetic ISEDs of the clusters. The differences between the ISED of the SSP component and the synthetic ISED of a cluster are exactly the BSs contributions. In this work, we are going to calculate such contributions for all the clusters in our sample in terms of both ISEDs and broadband colors.

3.1. ISED of Conventional SSP Model

In order to demonstrate the effect of BSs on the ISEDs of the conventional SSPs represented by OCs, the ISEDs of three clusters are given in Figure 3. The abscissa is the wavelength in angstrom, the ordinate is the integrated flux. The dotted line shows the ISED of BS component, the dash line shows that of the SSP component, and the solid line is the synthetic ISED of a cluster. It is clearly seen in Figure 3 that the ISEDs of the conventional SSPs have all been modified by BS components to some extent for all the clusters. In the left panel in Figure 3, normal stars still dominate, which means that the cluster’s ISED is determined by regular stars in that situation; while in the right panel, the synthetic ISED of the cluster is completely overwhelmed by the BS component.

The synthetic ISEDs show systematic enhancements towards shorter wavelengths due to addition of hotter stars (BSs) in the population, especially in UV and blue bands, which makes the ISEDs hotter than those of the conventional SSP model. The amplitudes of such modifications due to BS components depend on the detailed physical properties of both BSs and the host clusters, i.e., membership measurements, BSs positions in the CMDs, spatial configuration of the host clusters and the star richness of the clusters. All these things are crucial for the understanding of the real stellar populations containing stars with peculiar behaviors, like BSs discussed in our work. Detailed discussions on the scenario of BS property and its consequence on ISED of a population can be found in XD05.

3.2. Broadband color of conventional SSP model

Photometric observations, usually in broadband colors, are more frequently used than spectrophotometry when trying to understand stellar populations in remote galaxies in unresolvable conditions. Including of BS components in the conventional SSP model, the ISEDs are inclined to the UV and blue bands and consequently make the integrated (U-B) and (B-V) colors bluer. The use of these two colors is practically a good choice to show the photometric effect of BSs. This fact provides a quantitative way to measure the modification to the conventional SSP model. Bluer broadband colors in real stellar populations with respect to the conventional model at the same parameter can be misunderstood by EPS method with either younger ages or lower metallicities. Therefore, (U-B) and (B-V) colors are taken as detectors in this work to quantify BSs contributions to the conventional SSP model. The colors are obtained by convolving the ISEDs with corresponding filter responses.

As shown in Figure 4 and Figure 5, respectively, the (U-B) and (B-V) colors have been dramatically modified by BSs. These two figures are plotted using all the 97 sample OCs,

including the clusters without accurate metallicity measurements and assumed $Z=0.02$. The abscissa is the logarithmic ages of sample OCs. The ordinate is the broadband colors as indicated. The solid triangles are colors of the SSP components, and the open squares are colors of our sample OCs involving BSs contributions. In order to interpret BS influence on SSP in terms of color, we put a set of theoretical colors of SSP model as functions of age by lines in different types in each figure. In Figure 4, the five lines demonstrating the convectional SSP model in (U-B) are from BC03 in low-resolution case with different metallicities. In Figure 5, the five lines present the same fact as in figure 4 for (B-V) color with expanded ages so that uncertainty in age can be measured. The lines are given by keeping the invariable (B-V) color of SSP components (solid triangles) while expanding the ages for given values. For example, when keeping the same (B-V) color of each triangle point but changing the corresponding age by 0.1 dex larger than the original one, the solid line of “ $\log(\text{age})+0.1$ ” is plotted. Similarly, other lines are made with different age increments. Detailed number for each line is given in the figure.

As shown in Figure 4, the (U-B) colors of SSP components of younger ages (< 1.0 Gyr) stay close the theoretical line of BC03 of $Z=0.02$, while those of old ages (≥ 1.0 Gyr) have considerable deviations from that line. Such a pattern is not understood with the distribution in the Galactic plane and the history of formation and evolution of the clusters. However, it infers that for younger clusters, solar value is a good approximation if no accurate determination for metallicity is available. For the old clusters in the sample, the determination of metallicity is more reliable, therefore the spread may be due to true scatter in metallicity.

In contrast to the SSP components, the (U-B) and (B-V) colors of the clusters including BSs contributions scatter much larger in both age and metallicity plots (open squares in Figures 4 and 5). It is apparent that large differences will be expected when trying to get age and metallicity estimations for the clusters from the figures using the conventional SSP model. The theoretical colors described as different lines in these two figures cover the metallicity region from $Z=0.0001$ to $Z=0.02$ and the age region from “ $\log(\text{age})+0.1$ ” to “ $\log(\text{age})+0.5$ ”, but even such big enlargements of age or metallicity parameter can not completely interpret all the modified colors. It means that when trying to get the basic parameters of real stellar populations using broadband colors, the conventional SSP model can make the results very weird as we demonstrate for these OCs sample. Therefore we suggest that, in order to understand correctly stellar contents in various stellar systems, the results of stellar interactions, especially the bright BSs, should be implemented into the SSP model and EPS framework in a systematic way.

4. UNCERTAINTIES OF THE CURRENT CONVENTIONAL SSP MODEL

In previous section, it is shown that the ISEDs and broadband (U-B) and (B-V) colors of our sample OCs are dramatically modified by taking into account the BS populations. The modifications can introduce sizable uncertainties on the basic physical parameters of a stellar population if one keeps using the conventional SSP model. Taking a few clusters as example, it is possible to quantify these uncertainties. Focus is put on the uncertainties in age and metallicity in fitting the cluster’s ISED using that of conventional SSP model.

4.1. Fitting the synthetic ISEDs of OCs

One of the main effect of BSs is to make the synthetic ISEDs of our sample OCs hotter, i.e. the spectra get enhanced in UV and blue bands. The synthetic hotter (than the fitted isochrone can tell) ISEDs can still be well fitted with an SSP model of either younger age or lower metallicity than what is read from isochrone fitting in the CMD. Based on this, the synthetic ISEDs of our sample OCs are regarded as the real (observational) ones and are to be fitted by ISEDs of conventional SSP model with depressed ages or metallicities, and then the differences between cluster real parameters and fitting results can be used to discuss the fitting uncertainties that are potentially existing in all applications of the EPS scheme.

Taking NGC 2251 as an example, the best-fitting results are presented in Figure 6. In the two panels, the abscissa is the wavelength in angstrom. The ordinate is the logarithmic value of the absolute flux of ISED normalized at wavelength of 5500 Å. In the lower frames, the fitting residual δ between the synthetic ISED of the cluster and the best-fitting ISED of conventional SSP model is given, together with the standard deviation σ in the region of $\pm 3\sigma$ in dotted lines. The left panel presents the best-fitting result with metallicity untouched, but depressing the age parameter, while the right panel is that just the opposite, keeping the same age but depressing the metallicity. The synthetic ISED of the cluster is plotted in solid line. The ISED of conventional SSP model is shown by the dash line. As a comparison, the real parameters of the cluster are given in the top right corner in each panel. The parameters of the fitting model ISED are labeled below the fitted dash line.

As shown in Figure 6, if we let the parameter of age or metallicity free, conventional SSP model can fit perfectly most of the features of the synthetic ISED of the cluster, especially the whole optical region. In this case, the broadband photometry tells no difference. The main exception is focused on the extreme UV band, where the availability of observation and the accuracy of the theoretical model are both not perfect. That is to say, the conventional SSP model is certain to do good job on fitting the observational ISEDs of stellar populations,

but the fitting results indeed suffer great uncertainties, as shown by this example.

4.2. Fitting uncertainties in age

By doing the same fitting work for all the 97 sample OCs as what is done for NGC 2251 (Figure 6), the parameter differences between real cluster parameters (derived directly from fitting the resolved stars in CMD) and the fitting results (regarded as photometric measurements in unresolvable conditions) can then be collected to achieve the fitting uncertainties analysis.

Figure 7 demonstrates the age uncertainties. The abscissa is the logarithmic age values of our sample clusters from the best isochrone fitting results on the CMDs of the clusters. This is the most reliable age measurement and these ages can be regarded as the true ones, thus the abscissa is marked by $\log(\text{age})_{\text{true}}$. The ordinate is the age values made by fitting the synthetic ISEDs of our sample OCs with the ISEDs of conventional SSP model. It is marked by $\log(\text{age})_{\text{fit}}$. If these two ages of clusters were the same, all the points would stay in the diagonal line. The open squares show the age determinations by taken into account the BS components.

As shown in Figure 7, almost all the open squares locate below the diagonal, which means that when fitting the observed ISEDs of stellar populations (the synthetic ISED of a cluster) with the conventional SSP model, the ages will be systematically younger than the true ages as isochrone fitting from the photometric data. The dash line in Figure 7 shows the least square fitting results of all the open squares, which marks the uncertainties on average as the conventional SSP model can make in unresolved conditions. If we evaluate the underestimation level by the ratio of $(\log(\text{age})_{\text{true}} - \log(\text{age})_{\text{fit}})/\log(\text{age})_{\text{true}}$, the logarithmic age value underestimation goes from about 2% at $\log(\text{age})=8.5$, to 3% at $\log(\text{age})=9$ and 4% at $\log(\text{age})=9.5$ as shown in figure 7, becoming larger for older ages. The two well studied clusters, NGC 188 and NGC 2682 (M67), are marked in the plot with solid triangle and pentagon, respectively. As the BS populations are reliably know in them, their positions in the figure can be thought as calibrations of our method. Indeed, they agree quite well with our analysis.

4.3. Fitting uncertainties in metallicity

Figure 8 is for the analysis of metallicity uncertainty. The clusters with their BS contribution overwhelming are not used because the fitting results are obviously not realistic. On

the other hand, the BSs in these excluded clusters need more photometry and membership studies. The total number of 83 clusters are plotted in Figure 8. The abscissa (Z_{true}) is the true metallicities of sample OCs, also fixed by isochrone fitting technique using resolved photometric data. The ordinate (Z_{fit}) is the metallicity values made by fitting the synthetic ISEDs with those of conventional SSP model of lower metallicities. The open squares present metallicity values of two measurements. The solid circles are the results of the clusters without metallicity references and assumed $Z=0.02$ (entries in Table 1 marked “ $Z=0.02?$ ”). The short-dash line is again a least square fitting to data points with metallicity measurements, and the long-dash line is the least square fitting results of all the points (including solid circles). The short-dash line with metallicity measurements is used for the discussion below.

It is clearly shown in Figure 8 that vast majority of data points locate below the diagonal. In a similar way as for age analysis, the ratio of $(Z_{true}-Z_{fit})/Z_{true}$ is used to measure the uncertainty level, which goes from nearly 44% at $Z=0.008$ to 50% at $Z=0.02$. Again, NGC 188 and NGC 2682 (M67) are put in the plot as references.

Compared with isochrone fitting technique, spectra observation of individual stars is no doubt a more reliable way to get metallicity information of a star cluster. However, it still suffers some problems. The accuracy is connected with observational conditions, extinction and contamination effect. The results coming from that are also not perfectly ensured since the metallicity determination based on different stars in different regions in a cluster will produce different results, and due to selection effect, red giant branch stars in a cluster are easier taken as observational candidates than main sequence stars. Besides observational uncertainties, theoretical model is another uncertainty source for this statistic results, since there are originally only limited metallicity grids from both theoretical evolutionary tracks (Bressan et al. 1994) and model atmospheres (Lejeune et al. 1997). Stellar spectra used for synthetic ISEDs of clusters rely heavily on interpolation. Therefore, the metallicity uncertainties presented in Figure 8 should be considered as qualitative statistic results. More significant movements on this problem should be supported by more reliable observational data and more detailed model calculations.

5. CONCLUSIONS

As a follow-up work of XD05, the main aim of this work is to extend the study to larger sample and to quantify the influence of BSs on the conventional SSP model. With a sample of 97 Galactic OCs of ages ≥ 0.1 Gyr, we confirm the results of XD05 that the integrated spectral properties OCs are dramatically modified by the BS contents in the clusters. The ISEDs are greatly enhanced towards shorter wavelength, becoming significantly bluer, and

consequently the broadband (U-B) and (B-V) colors are modified accordingly. When the conventional SSP model is adopted in understanding stellar contents in galaxies, either using spectra or broadband colors, great uncertainties in age and/or metallicity will be brought in.

Directly fitting the synthetic ISEDs of our sample OCs with the ISEDs of conventional SSP model can still result in nice fittings, if one lets the parameter of age or metallicity free. But the fitting parameters have significant underestimations when compared with the true parameters made photometrically. In the parameter regions covered by our sample OCs, the logarithmic age value underestimation rates ranges 2% at $\log(\text{age})=8.5$, 3% at $\log(\text{age})=9.0$ and 4% at $\log(\text{age})=9.5$. There is a trend for such a ratio to become larger for greater ages. Also due to the presence of BSs in real stellar populations, the metallicity parameter can also be seriously underestimated by conventional SSP models. This is true at least qualitatively within the scope of current work due to the uncertainties in measuring the metallicity independently by other means.

Taking OCs as general representatives of SSPs in galaxies, and limiting our results to the age and metallicity ranges covered by the working sample of current work, the conventional SSP model derived from the single star evolution theory is seriously altered by the descendants of stellar interactions that are presumably common in normal environments. BSs discussed in our work are the most important components that are proved to be widely existing in all stellar systems (Stryker 1993). Therefore, the effect of BSs must be taken into account when EPS technique is applied to study the properties of stellar populations in galaxies.

Theoretical refinery of the conventional SSP model still needs more studies. Thorough investigations of several issues should be put forward, that including: the individual processes of stellar interactions including binary and multiple systems and the overall consequences of all these interactions to the population statistically, and effects of dynamical evolution of the stellar systems. Before such SSP model eventually become available, empirically corrected models would be a good practice. Based no current knowledge of interactive binary evolution and collisional processes, and the observational cluster data base, such models can be made. Work to this purpose is now in progress.

We would like to thank the Chinese National Science Foundation for support through grants 10573022, 10333060, 10521001 and 10433030.

Table 1. Parameters of the Sample Clusters

Cluster Name	$\log(\text{age})$	$E(B-V)$	DM	Z	[Fe/H]	N_2	N_{BS}	Ref.
Berkeley 11	8.04	0.95	11.71	0.02?	...	15	1	1,2
Berkeley 32	9.80	0.08	12.60	0.012	-0.20	150	19	2,3
Berkeley 39	9.78	0.11	13.60	0.01	-0.31	220	29	2,4,5
Berkeley 42	9.32	0.76	11.31	0.02?	...	20	1	1,2
Blanco 1	8.32	0.01	7.18	0.035	0.23	10	1	1,2,6
Collinder 223	8.00	0.25	13.00	0.02?	...	25	2	2,7
Hyades	8.80	0.01	3.39	0.029	0.15	40	1	2,8
IC 166	9.00	0.80	15.65	0.02	0.00	110	11	2,9,10
IC 1311	8.95	0.45	14.10	0.02	0.00	100	7	2,11
IC 1369	9.16	0.57	11.59	0.02?	...	35	6	1,2,8
IC 2488	8.25	0.24	11.20	0.019	-0.02	10	1	2,12
IC 2714	8.50	0.36	11.68	0.015	-0.12	80	1	2,13
IC 4651	9.23	0.10	10.03	0.025	0.10	35	8	2,14
IC 4756	8.90	0.23	7.60	0.022	0.04	55	1	2,15
King 2	9.78	0.31	13.80	0.02?	...	250	30	1,2
King 8	8.62	0.58	14.03	0.007	-0.46	35	5	1,2
King 11	9.70	1.00	11.70	0.011	-0.27	140	24	1,2,16
Melotte 66	9.65	0.16	13.75	0.006	-0.53	180	46	2,17
Melotte 105	8.40	0.52	11.80	0.02?	...	25	1	2,18
Melotte 111	8.60	0.00	4.77	0.019	-0.03	10	1	2,19
NGC 188	9.85	0.08	11.35	0.019	-0.01	170	20	2,20
NGC 381	8.77	0.34	11.18	0.024	0.07	25	1	1,2,6
NGC 752	9.14	0.04	8.43	0.016	-0.09	25	1	1,2,6
NGC 1027	8.55	0.33	10.46	0.023	0.06	40	2	2,6,8
NGC 1193	9.90	0.12	13.80	0.01	-0.29	190	16	2,21
NGC 1245	9.02	0.29	12.27	0.018	-0.05	75	9	2,22,23
NGC 1252	9.48	0.02	9.04	0.02?	...	7	1	1,2
NGC 1342	8.65	0.32	10.11	0.014	-0.16	20	4	1,2,6
NGC 1528	8.57	0.30	10.19	0.011	-0.27	35	3	2,6,8
NGC 1545	8.45	0.30	10.19	0.017	-0.06	20	1	1,2,6
NGC 1664	8.47	0.25	11.17	0.029	0.15	30	4	1,2,6,8
NGC 1778	8.18	0.23	11.53	0.02?	...	15	1	2,6
NGC 1817	9.05	0.19	10.90	0.009	-0.34	35	7	2,24

Table 1—Continued

Cluster Name	log(age)	E(B-V)	DM	Z	[Fe/H]	N ₂	N _{BS}	Ref.
NGC 1901	8.93	0.02	8.12	0.02?	...	10	1	2,6
NGC 1912	8.56	0.25	10.91	0.015	-0.11	45	3	2,6,25
NGC 2099	8.81	0.23	11.50	0.011	-0.25	120	8	2,26
NGC 2168	8.30	0.255	9.60	0.012	-0.21	70	13	2,27,28
NGC 2204	9.40	0.08	13.10	0.007	-0.44	180	9	2,29
NGC 2236	8.54	0.48	12.33	0.017	-0.07	10	2	1,2,8
NGC 2243	9.58	0.055	13.15	0.005	-0.57	120	7	2,30
NGC 2251	8.48	0.21	11.21	0.012	-0.20	15	3	2,6,31
NGC 2266	8.80	0.10	12.95	0.011	-0.26	45	2	2,32
NGC 2281	8.70	0.06	8.92	0.027	0.13	35	3	1,2,6
NGC 2287	8.39	0.03	9.30	0.022	0.04	30	3	1,2,6
NGC 2301	8.31	0.03	9.76	0.023	0.06	15	1	1,2,6
NGC 2324	8.65	0.25	13.70	0.008	-0.40	70	8	2,33
NGC 2354	9.00	0.13	10.80	0.01	-0.30	100	5	2,34
NGC 2360	9.08	0.08	10.50	0.014	-0.15	25	4	1,2,35,36
NGC 2383	8.60	0.22	13.30	0.02?	...	5	1	2,25
NGC 2395	9.18	0.07	8.91	0.02?	...	12	1	2,8,37
NGC 2420	9.30	0.05	11.95	0.009	-0.32	140	12	2,38
NGC 2422	8.12	0.07	8.67	0.02?	...	5	1	2,6
NGC 2437	8.39	0.15	11.16	0.023	0.06	70	5	1,2,6
NGC 2477	9.00	0.30	10.50	0.018	-0.05	190	28	2,39
NGC 2506	9.25	0.04	12.60	0.012	-0.20	130	12	2,40,41,42
NGC 2516	8.15	0.12	7.93	0.018	-0.05	35	6	2,43
NGC 2533	8.88	0.05	12.64	0.02?	...	30	1	1,2
NGC 2539	8.80	0.06	10.60	0.018	-0.04	20	1	2,44,45
NGC 2632	8.90	0.01	6.39	0.028	0.14	30	5	1,2,6
NGC 2660	9.00	0.40	12.20	0.02	0.00	110	18	2,11
NGC 2682	9.60	0.038	9.65	0.018	-0.04	200	30	2,46
NGC 2818	8.70	0.22	12.90	0.02?	...	45	5	2,47
NGC 3114	8.48	0.07	9.80	0.02?	...	50	5	2,48
NGC 3496	8.78	0.52	10.70	0.02?	...	70	4	2,49
NGC 3532	8.54	0.04	8.59	0.019	-0.02	90	9	2,50,51
NGC 3680	9.27	0.06	10.20	0.014	-0.14	18	4	2,52

Table 1—Continued

Cluster Name	$\log(\text{age})$	$E(B-V)$	DM	Z	[Fe/H]	N_2	N_{BS}	Ref.
NGC 3960	8.95	0.29	11.60	0.015	-0.12	50	4	2,53
NGC 4349	8.32	0.38	12.87	0.015	-0.12	25	1	1,2,6
NGC 5316	8.19	0.27	11.26	0.019	-0.02	20	4	1,2,6
NGC 5460	8.30	0.144	9.49	0.02?	...	20	1	2,54
NGC 5617	8.15	0.54	11.53	0.02?	...	70	9	2,55
NGC 5822	9.08	0.15	9.85	0.014	-0.15	80	6	2,56
NGC 5823	8.90	0.50	10.50	0.016	-0.10	35	1	2,6,57
NGC 6067	8.11	0.32	11.17	0.021	0.01	60	7	2,58
NGC 6208	9.00	0.18	10.00	0.019	-0.03	60	5	1,2,59
NGC 6259	8.34	0.68	11.50	0.025	0.10	85	3	1,2,60,61
NGC 6281	8.51	0.15	8.93	0.02	0.00	25	4	1,2,6
NGC 6416	8.78	0.25	10.12	0.02?	...	35	3	2,6
NGC 6475	8.34	0.07	7.30	0.022	0.03	15	2	1,2,62
NGC 6633	8.80	0.17	7.80	0.015	-0.11	40	3	2,15
NGC 6705	8.40	0.38	12.70	0.028	0.14	110	1	1,2,6,8
NGC 6791	10.08	0.09	12.79	0.04	0.30	110	27	2,63
NGC 6802	8.87	0.85	10.25	0.007	-0.45	35	7	1,2,64
NGC 6819	9.40	0.10	11.80	0.024	0.07	270	33	2,65
NGC 6866	8.68	0.17	11.33	0.025	0.10	35	1	2,6,8
NGC 6939	9.11	0.34	11.30	0.02?	...	80	4	2,66
NGC 6940	8.94	0.21	10.08	0.021	0.01	130	7	1,2,6
NGC 7031	8.14	0.85	9.77	0.02?	...	15	1	1,2
NGC 7039	8.83	0.18	11.30	0.02?	...	35	1	2,6,8
NGC 7062	8.70	0.42	12.76	0.02?	...	35	2	2,67
NGC 7063	8.42	0.09	9.47	0.014	-0.16	15	1	2,6,8
NGC 7142	9.65	0.35	11.40	0.016	-0.10	120	23	2,68
NGC 7789	9.20	0.25	12.21	0.013	-0.18	130	25	2,69
Ruprecht 97	9.00	0.21	13.70	0.02?	...	12	1	2,70
Ruprecht 98	8.78	0.16	9.42	0.02?	...	7	1	2,6
Ruprecht 108	8.41	0.14	10.21	0.02?	...	5	1	2,6
Tombaugh 1	9.11	0.30	12.70	0.01	-0.30	5	1	2,71

References. — 1: Dias et al. 2002, 2: Ahumada & Lapasset 1995, 3: Richtler & Sagar 2001, 4: Carraro et al. 1994, 5: Friel & Janes 1993, 6: Kharchenko et al. 2005, 7: Tadross 2004, 8: Loktin et al. 1994, 9: Vallenari et al. 2000, 10: Manteiga et al. 1995, 11: Bragaglia et al. 2000, 12: Clariá et al. 2003, 13: Clariá et al. 1994, 14: Meibom et al. 2002, 15: Hebb et al. 2004, 16: Aparicio et al. 1991, 17: Twarog et al. 1995, 18: Sagar et al. 2001, 19: van Leeuwen 1999, 20: Krusberg & Chaboyer 2006, 21: Kaluzny 1988, 22: Burke et al. 2004, 23: Subramaniam 2003, 24: Balaguer-Núñez et al. 2004, 25: Subramaniam & Sagar 1999, 26: Kalirai et al. 2005, 27: Barrado y Navascués et al. 2001, 28: Sung & Bessell 1999, 29: Frogel & Twarog 1983, 30: Anthony-Twarog et al. 2005, 31: Celeste Parisi et al. 2005, 32: Kaluzny & Mazur 1991, 33: Piatti et al. 2004a, 34: Clariá et al. 1999, 35: Mermilliod & Mayor 1990, 36: Murray et al. 1988, 37: Zdanavičius et al. 2004, 38: Lee et al. 2002, 39: Eigenbrod et al. 2004, 40: Carretta et al. 2004, 41: Kim et al. 2001, 42: Marconi et al. 1997, 43: Terndrup et al. 2002, 44: Marshall et al. 2005, 45: Lapasset et al. 2000, 46: VandenBerg & Stetson 2004, 47: Surendiranath et al. 1990, 48: Carraro & Patat 2001, 49: Balona & Laney 1995, 50: Eggen 1981, 51: Sarajedini et al. 2004, 52: Anthony-Twarog et al. 2004, 53: Bragaglia et al. 2006, 54: Barrado & Byrne 1995, 55: Ahumada 2005, 56: Twarog et al. 1993, 57: Janes 1981, 58: Luck 1994, 59: Paunzen & Maitzen 2001, 60: Mermilliod et al. 2001, 61: Anthony-Twarog et al. 1989, 62: Prosser et al. 1996, 63: Stetson et al. 2003, 64: Sirbaugh et al. 1995, 65: Kang & Ann 2002, 66: Andreuzzi et al. 2004, 67: Freyhammer et al. 2001, 68: Crinklaw & Talbert 1991, 69: Bartašiutė & Tautvaišienė 2004, 70: van den Bergh et al. 1976, 71: Piatti et al. 2004b

REFERENCES

- Ahumada, J. A. 2005, AN, 326, 3
- Ahumada, J., & Lapasset, E. 1995, A&AS, 109, 375 (AL95)
- Andreuzzi, G., Bragaglia, A., Tosi, M., Marconi, G. 2004, MNRAS, 348, 297
- Anthony-Twarog, B. J., Atwell, J., Twarog, B. A. 2005, AJ, 129, 872
- Anthony-Twarog, B. J., Payne, D. M., Twarog, B. A. 1989, AJ, 97, 1048
- Anthony-Twarog, B. J., Twarog, B. A. 2004, AJ, 127, 1000
- Aparicio, A., Bertelli, C., Chiosi, C., Garcia-Pelayo, J. M. 1991, ASPC, 13, 230
- Balaguer-Núñez, L., Jordi, C., Galadí-Enríquez, D., Zhao, J. L. 2004, A&A, 426, 819
- Balona, L. A., Laney, C. D. 1995, MNRAS, 277, 250
- Barrado, D., Byrne, P. B. 1995, A&AS, 111, 275
- Battinelli, P., Brandimarti, A., Capuzzo-Dolcetta, R. 1994, A&AS, 104, 379
- Bartašiutė, S., Tautvaišienė, G. 2004, Ap&SS, 294, 225
- Bertelli, G., Bressan, A., Chiosi, C., Fagotto, F., Nasi, E. 1994, A&AS, 106, 275
- Bica, E., Alloin, D. 1986a, A&AS, 66, 171
- Bica, E., Alloin, D. 1986b, A&A, 162, 21
- Bragaglia, A., Tosi, M., Carretta, E., Gratton, R. G., Marconi, G., Pompei, E. 2006, MNRAS, 366, 1493
- Bragaglia, A., Tosi, M., Marconi, G., Sandrelli, S. 2000, ASPC, 198, 51
- Bressan, A., Chiosi, C., Fagotto, F. 1994, ApJS, 94, 63
- Bruzual G., Charlot, S. 2003, MNRAS, 344, 1000 (BC03)
- Burke, C. J., Gaudi, B. S., DePoy, D. L., Pogge, R. W., Pinsonneault, M. H. 2004, AJ, 127, 2382
- Carraro, G., Chiosi, C., Bressan, A., Bertelli, G. 1994, A&AS, 103, 375
- Carraro, G., Patat, F. 2001, A&A, 379, 136
- Carretta, E., Bragaglia, A., Gratton, R. G., Tosi, M. 2004, A&A, 422, 951

- Celeste Parisi, M., Clariá, J. J., Piatti, A. E., Geisler, D. 2005, MNRAS, 363, 1247
- Chen, X. F., Han, Z. W. 2004, MNRAS, 355, 1182
- Clariá, J. J., Mermilliod, J.-C., Piatti, A. E. 1999, A&AS, 134, 301
- Clariá, J. J., Minniti, D., Piatti, A. E., Lapasset, E. 1994, MNRAS, 268, 733
- Clariá, J. J., Piatti, A. E., Lapasset, E., Mermilliod, J.-C. 2003, A&A, 399, 543
- Crinklaw, G., Talbert, F. D. 1991, PASP, 103, 536
- Deng, L., Chen, R., Liu, X. S., Chen, J. S. 1999, ApJ, 524, 824
- Dias, W. S., Alessi, B. S., Moitinho, A., Lépine, J. R. D. 2002, A&A, 389, 871
- Eggen, O. J. 1981, ApJ, 246, 817
- Eigenbrod, A., Mermilliod, J.-C., Clariá, J. J., Andersen, J., Mayor, M. 2004, A&A, 423, 189
- Ferraro, F. R., Sills, A., Rood, R. T., Paltrinieri, B., Buonanno, R. 2003, ApJ, 588, 464
- Freyhammer, L. M., Arentoft, T., Sterken, C. 2001, A&A, 368, 580
- Friel, E. D., Janes, K. A. 1993, A&A, 267, 75
- Frogel, J. A., Twarog, B. A. 1983, ApJ, 274, 270
- Hebb, L., Wyse, R. F. G., Gilmore, G. 2004, AJ, 128, 2881
- Hurley, J. R., Pols, O. R., Aarseth, S. J., Tout, C. A. 2005, MNRAS, 363, 293
- Janes, K. A. 1981, AJ, 86, 1210
- Kaluzny, J. 1988, AcA, 38, 339
- Kaluzny, J., Mazur, B. 1991, AcA, 41, 191
- Kang, Y.-W., Ann, H. B. 2002, JKAS, 35, 87
- Kharchenko, N. V., Piskunov, A. E., Röeser, S., Schilbach, E., Scholz, R.-D. 2005, A&A, 438, 1163
- Kim, S.-L., Chun, M.-Y., Park, B.-G., Kim, S. C., Lee, S. H., Lee, M. G., Ann, H. B., Sung, H., Jeon, Y.-B., Yuk, I.-S. 2001, AcA, 51, 49
- Krusberg, Z. A. C., Chaboyer, B. 2006, AJ, 131, 1565
- Lapasset, E., Clariá, J. J., Mermilliod, J.-C. 2000, A&A, 361, 945

- Lee, M. G., Park, H. S., Park, J.-H., Sohn, Y.-J., Oh, S. J., Yuk, I.-S., Rey, S.-C., Lee, S.-G., Lee, Y.-W., Kim, H.-I., and 5 coauthors 2003, *AJ*, 126, 2840
- Lee, S. H., Ann, H. B., Kang, Y.-W. 2002, *aprm.conf*, 273
- Lejeune, Th., Cuisinier, F., Buser, R. 1997, *A&AS*, 125, 229
- Loktin, A. V., Matkin, N. V. 1994, *A&AT*, 4, 153
- Luck, R. E. 1994, *ApJS*, 91, 309
- Manteiga Outeira, M., Acarreta Rodriguez, J. R., Martinez Roger, C., Straniero, O. 1995, *IAUS*, 164, 377
- Marconi, G., Hamilton, D., Tosi, M., Bragaglia, A. 1997, *MNRAS*, 291, 763
- Marshall, J. L., Burke, C. J., DePoy, D. L., Gould, A., Kollmeier, J. A. 2005, *AJ*, 130, 1916
- Meibom, S., Andersen, J., Nordström, B. 2002, *A&A*, 386, 187
- Mermilliod, J.-C., Clariá, J. J., Andersen, J., Piatti, A. E., Mayor, M. 2001, *A&A*, 375, 30
- Mermilliod, J.-C., Mayor, M. 1990, *A&A*, 237, 61
- Murray, R. L., Anthony-Twarog, B. J., Twarog, B. A. 1988, *BAAS*, 20, 717
- Paunzen, E., Maitzen, H. M. 2001, *A&A*, 373, 153
- Piatti, A. E., Clariá, J. J., Ahumada, A. V. 2004a, *A&A*, 418, 979
- Piatti, A. E., Clariá, J. J., Ahumada, A. V. 2004b, *A&A*, 421, 991
- Piotto, G., King, I. R., Djorgovski, S. G., Sosin, C., Zoccali, M., Saviane, I., De Angeli, F., Riello, M., Recio Blanco, A., Rich, R. M., Meylan, G., Renzini, A. 2002, *A&A*, 391, 945
- Pols, O. R., Marinus, M. 1994, *A&A*, 288, 475
- Prosser, C. F., Randich, S., Stauffer, J. R. 1996, *AJ*, 112, 649
- Richtler, T., Sagar, R. 2001, *BASI*, 29, 53
- Sagar, R., Munari, U., de Boer, K. S. 2001, *MNRAS*, 327, 23
- Salpeter, E. E. 1955, *ApJ*, 121, 161
- Sandage, A. R. 1953, *AJ*, 58, 61
- Sarajedini, A., Brandt, K., Grocholski, A. J., Tiede, G. P. 2004, *AJ*, 127, 991

- Sirbaugh, R. D., Lewis, K. A., Friel, E. D. 1995, AAS, 18710708
- Stetson, P. B., Bruntt, H., Grundahl, F. 2003, PASP, 115, 413
- Stryker, L. L. 1993, PASP, 105, 1081
- Subramaniam, A. 2003, BASI, 31, 49
- Subramaniam, A., Sagar, R. 1999, AJ, 117, 937
- Surendiranath, R., Kameswara Rao, N., Sagar, R., Nathan, J. S., Ghosh, K. K. 1990, JApA, 11, 151
- Tadross, A. L. 2004, ChJAA, 4, 67
- Terndrup, D. M., Pinsonneault, M., Jeffries, R. D., Ford, A., Stauffer, J. R., Sills, A. 2002, ApJ, 576, 950
- Tian, B., Deng, L., Han, Z., Zhang, X. B. 2006, A&A, 455, 247
- Twarog, B. A., Anthong-Twarog, B. J., Hawarden, T. G. 1995, PASP, 107, 1215
- Twarog, B. A., Anthong-Twarog, B. J., McClure, R. D. 1993, PASP, 105, 78
- van den Bergh, S., Herbst, E., Harris, G. L., Herbst, W. 1976, ApJ, 208, 770
- van Leeuwen, F. 1999, ASPC, 167, 52
- Vallenari, A., Carraro, G., Richichi, A. 2000, A&A, 353, 147
- VandenBerg, D. A., Stetson, P. B. 2004, PASP, 116, 997
- Xin, Y., Deng, L. 2005, ApJ, 619, 824 (XD05)
- Zdanavicius, J., Zdanavicius, K., Straizys, V., Kazlauskas, A., Cernis, K., Chen, C. W., Chen, W. P., Boyle, R. P., Tautvaisiene, G. 2004, Balt.A, 13, 555

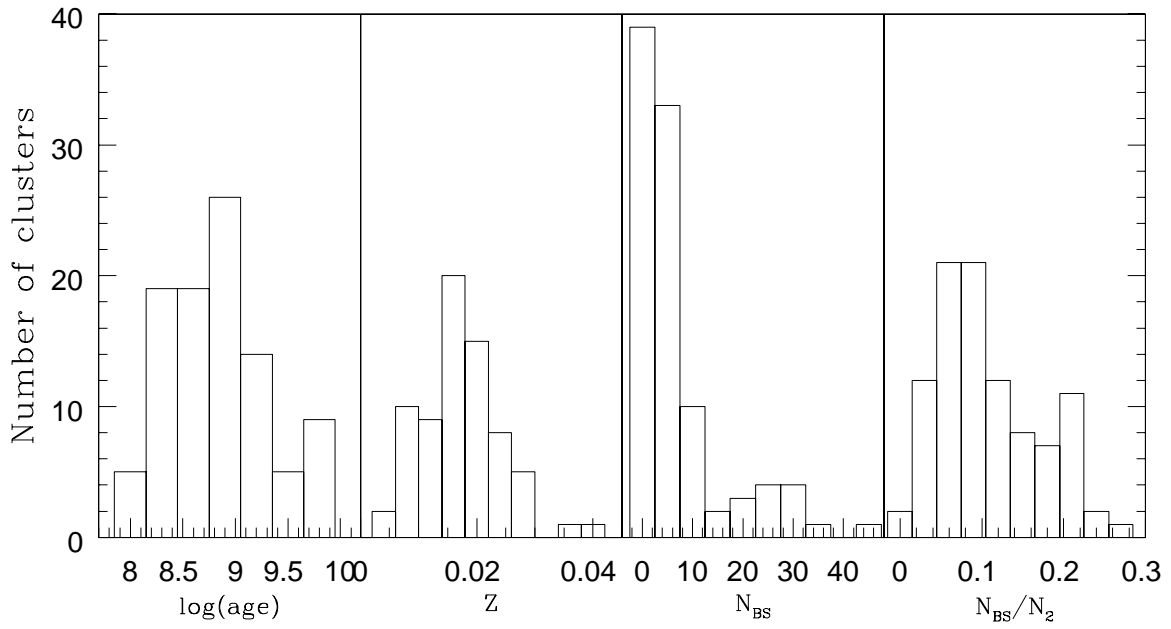


Fig. 1.— Number distributions of the sample OCs according to four different parameters: $\log(\text{age})$, Z , N_{BS} and N_{BS}/N_2 .

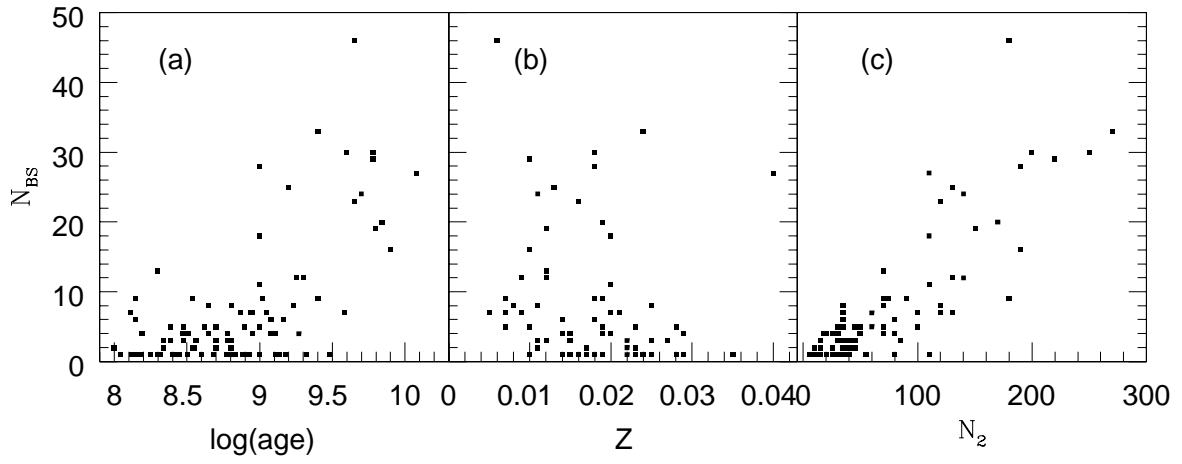


Fig. 2.— N_{BS} distributions according to three different parameters: $\log(\text{age})$, Z and N_2 .

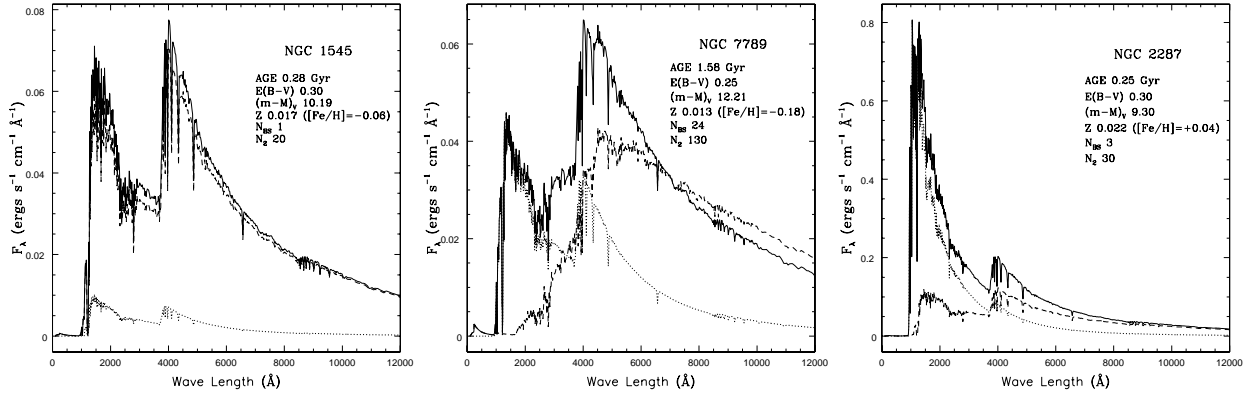


Fig. 3.— ISED modifications. *Dotted line* : ISED of the BS component. *Dash line* : ISED of the SSP component. *Solid line* : Synthetic ISED of the cluster.

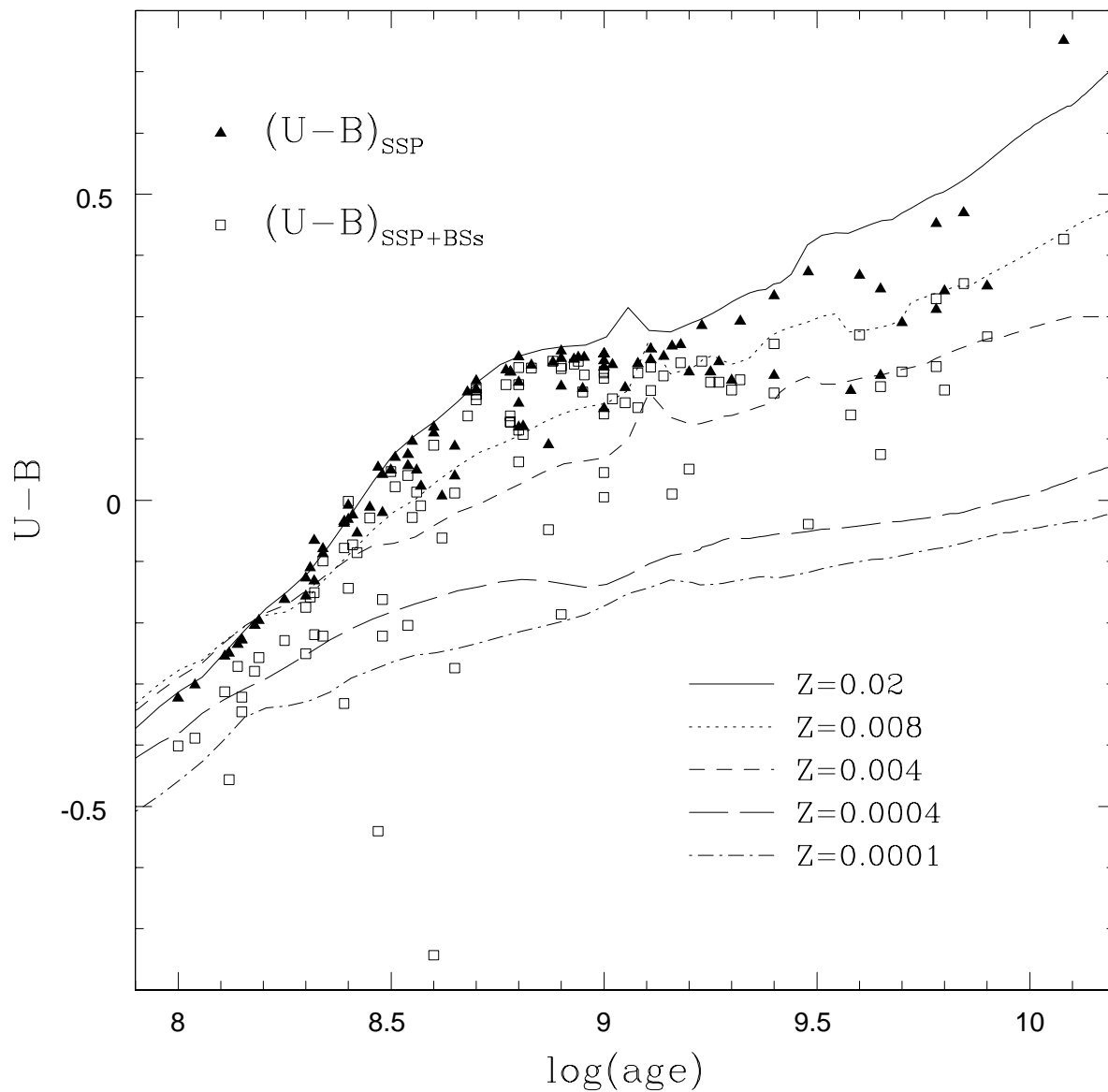


Fig. 4.— $(U-B)$ colors modified by BSs. The *Solid triangles* are $(U-B)$ colors of the SSP components. The *Open squares* are $(U-B)$ colors of our sample OCs including BS contributions. Five lines in different types are the theoretical $(U-B)$ colors from BC03 of different metallicities.

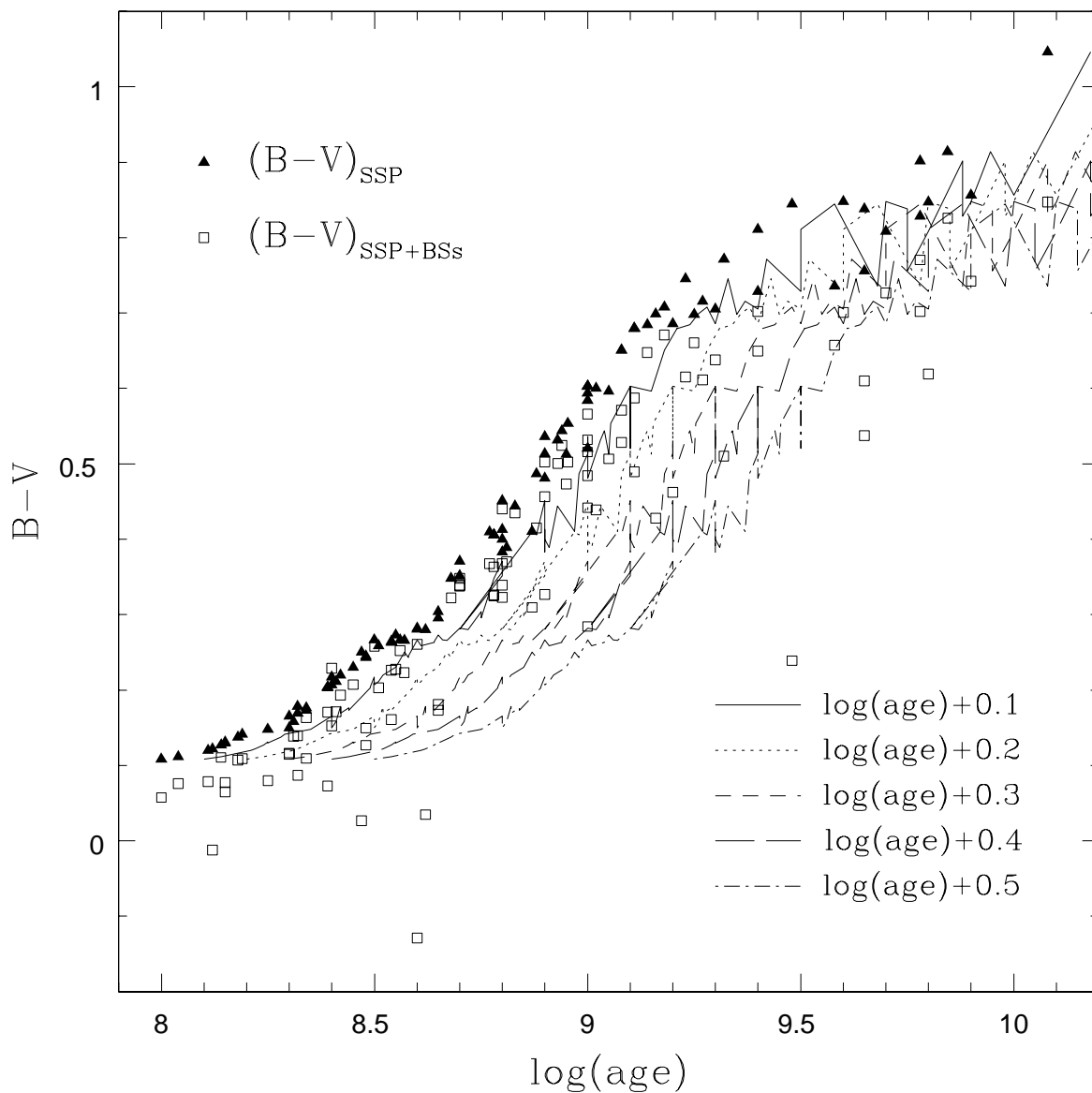


Fig. 5.— $(B-V)$ colors modified by BSs. The *Solid triangles* are $(B-V)$ colors of the SSP components. The *Open squares* are $(B-V)$ colors of our sample OCs including BS contributions. Five lines in different types are plotted by keeping the theoretical colors the same while expanding the ages, see text in details.

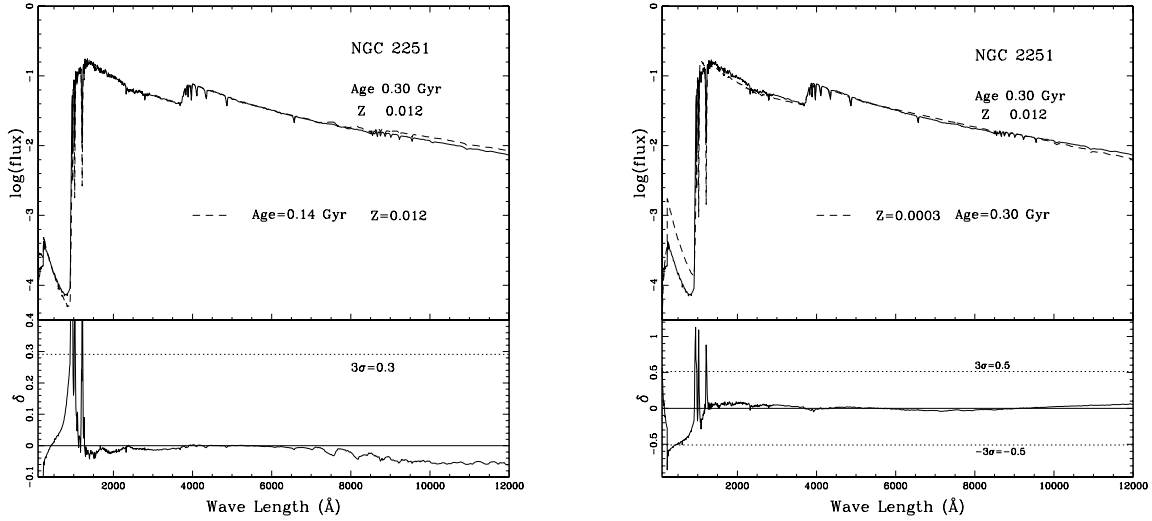


Fig. 6.— Fitting the synthetic ISED of NGC 2251 with the conventional SSP model. The abscissa is the wavelength in angstrom. The ordinate is the logarithmic value of cluster ISED normalized at 5500 \AA . δ is the differences between the synthetic and the conventional ISEDs. Standard deviation σ of δ is given in *dotted lines* in $\pm 3\sigma$. The left panel is the fitting result of keeping the same metallicity but depressing age. The right panel is the opposite, keeping the same age but lowering metallicity. The synthetic ISED is plotted in *solid line*. The conventional ISED is given in *dash line*. The real parameters of the cluster are listed in the top right corner in each panel. The parameters of the theoretical ISED are given below the fitting line.

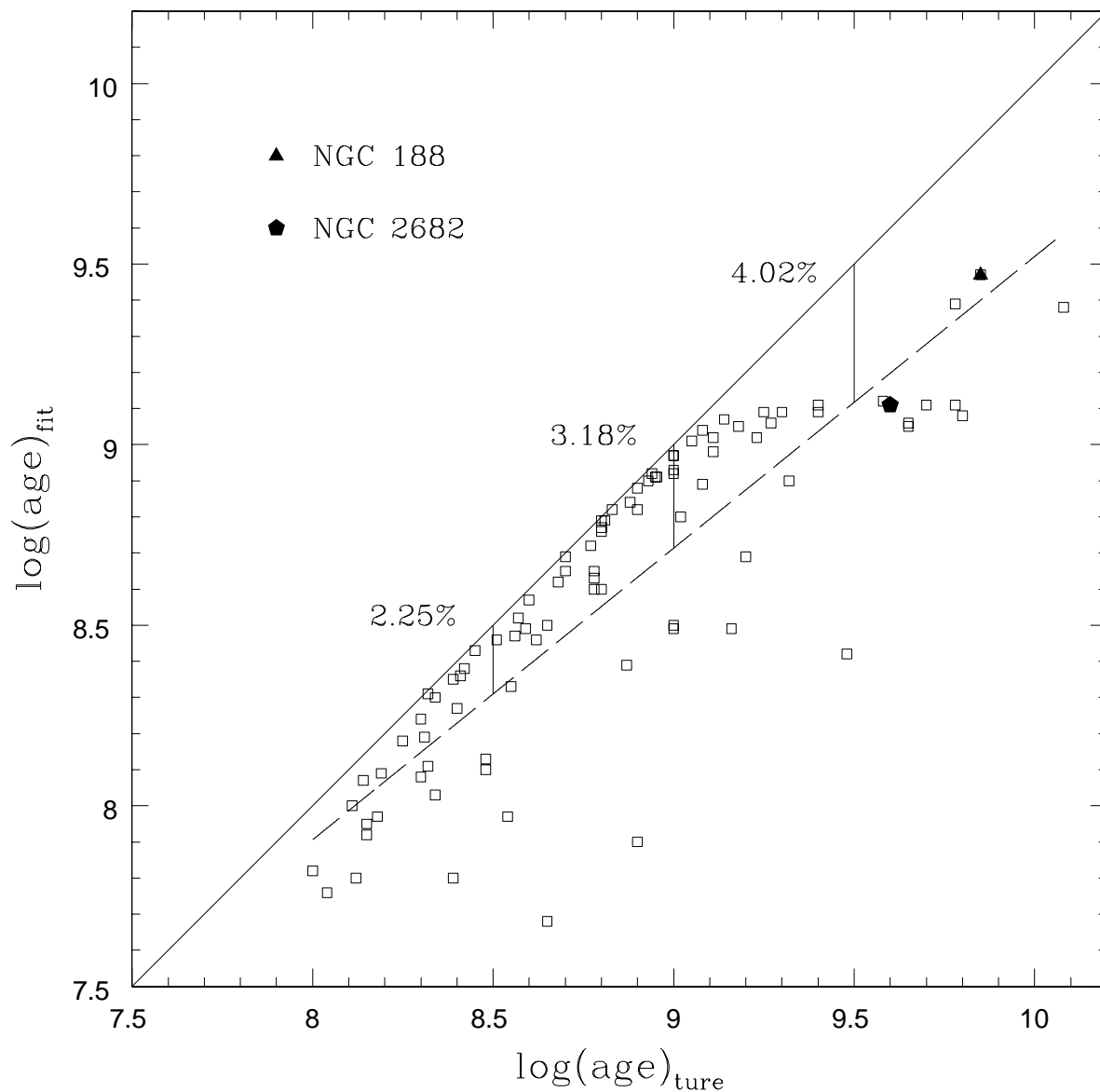


Fig. 7.— Fitting uncertainty in age. The abscissa is the real age of the cluster. The ordinate is the fitting age by the conventional SSP model. *Open squares* present age differences with and without the BS contributions. *Dash line* is the least square fitting results of all the *open squares*. Results for NGC 188 and NGC 2682 (M67) are marked by *solid triangle* and *solid pentagon*, respectively.

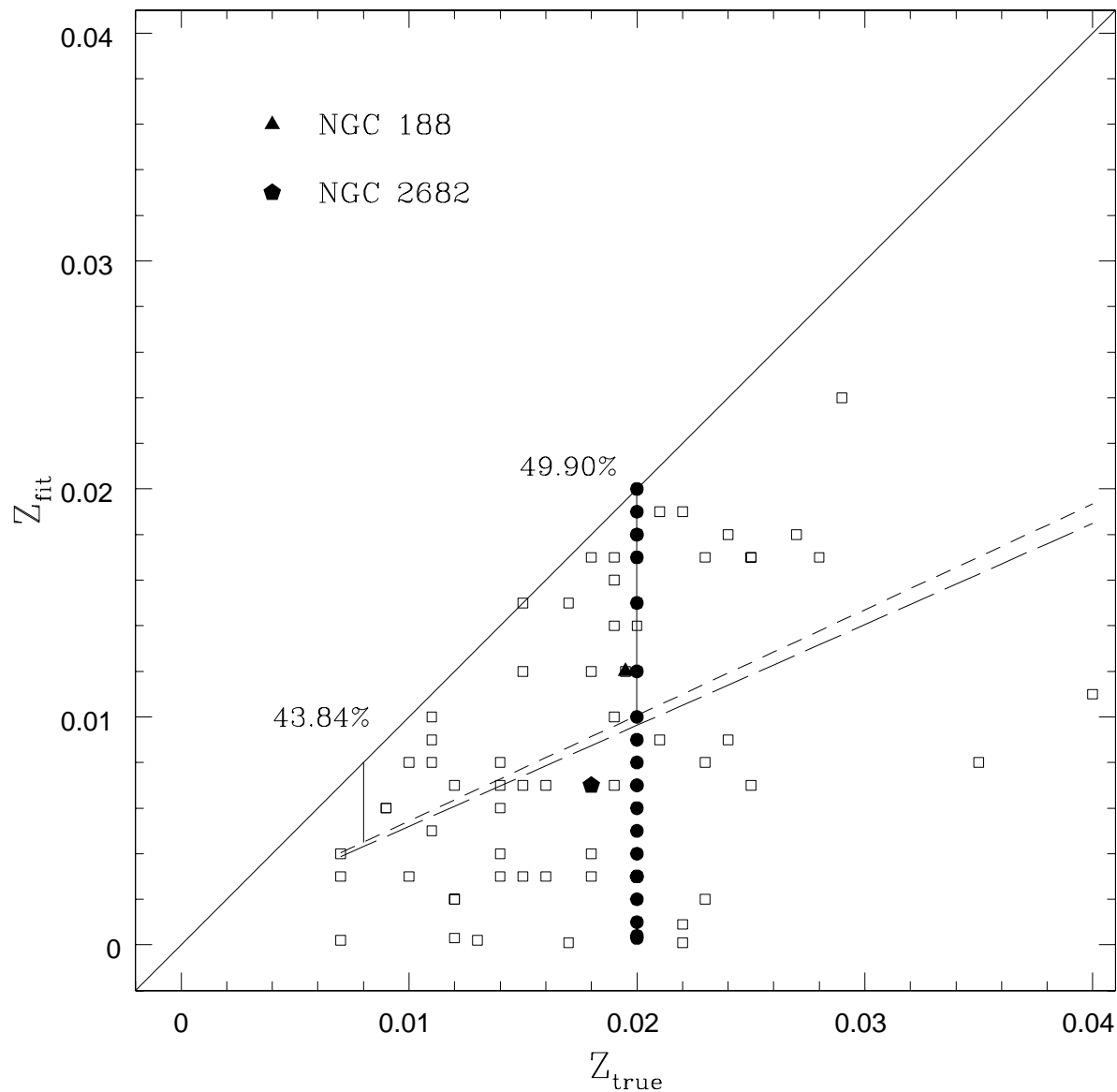


Fig. 8.— Fitting uncertainty in metallicity. The abscissa is the real metallicity of the cluster. The ordinate is the fitting metallicity by the conventional SSP model. *Open squares* present differences in metallicity with and without the BS contributions. *Solid circles* are results of those OCs assuming $Z=0.02$. *Short dash line* is the least square fitting results of all the *Open squares*. *Long Dash line* is the least square fitting results of all points. Results for NGC 188 and NGC 2682 (M67) are marked by *solid triangle* and *solid pentagon*, respectively.